Int. J. Appl. Comput. Math (2019) 5:48
https://doi.org/10.1007/s40819-019-0632-0

ORIGINAL PAPER

Boundary-Layer Separations of Mixed Convection Flow Past an Isothermal Circular Cylinder

Nepal Chandra Roy[1] · Tajnin Rahman[1] · Salaika Parvin[1]

Published online: 4 April 2019

Abstract
This study reveals the boundary-layer separations of unsteady mixed convection flow of incompressible fluid past a circular cylinder which is kept at a constant temperature. The governing equations are made dimensionless using an appropriate transformation. These equations are solved with the use of finite difference method. We also solve the problem using perturbation method for small time and local non-similarity method for long time. Results show that numerical solutions agree well with the series solutions obtained by perturbation method for small time and asymptotic method for long time. For an increase of Richardson number and Prandtl number, the local friction factor and the rate of heat transfer increases. Besides, the streamlines and isotherms reveal that when the Richardson number and the Prandtl number are increased, the point of separation of boundary-layer reduces and the size of vortex decreases. Moreover, the larger values of Richardson number thicken the thermal boundary layer whereas the reverse characteristic is observed for higher Prandtl numbers.

Keywords Boundary-layer separation · Mixed convection · Circular cylinder

Introduction

Mixed convection flow around a cylinder has a great importance due to its many real-life applications such as geothermal power generation, thermal design of buildings, electronics cooling, solar collectors, drilling operations, and float glass production. In particular, when the free convection flow is of same order of the forced convection flow, then the mixed convection flow must be considered. In order to circumvent the unpredictable damage of practical applications, it is vital to have a detailed knowledge about the flow and heat transfer of mixed convection around a cylinder. Because of a variety of applications, it requires a good deal effort to explore the characteristics of heat and momentum transfer from the cylinder placed in an incompressible fluid.

A theoretical analysis of the problem of mixed convection flow over solid bodies was performed by Acrivos [1]. Results are elucidated with the local Nusselt number when the Prandtl number, Pr, tends to zero as well as when Pr tends to infinity. Sparrow and Lee [2] investi-

✉ Nepal Chandra Roy
nepal@du.ac.bd

[1] Department of Mathematics, University of Dhaka, Dhaka 1000, Bangladesh

gated the mixed convection about a horizontal cylinder. Merkin [3] theoretically examined the oscillatory free convection flow from a horizontal cylinder. Also, Merkin [4] considered mixed convection flow from a horizontal cylinder which is flowing in the upward direction and showed that the heating cylinder delays separation. When the cylinder surface is assumed to be cooled, the point of separation occurs adjacent to the lower stagnation point. It has been reported that the boundary layer concept is not applicable for a sufficiently cooled cylinder surface. He discussed the flow regime according to the value of dimensionless buoyancy parameter, λ, defined as Richardson number and obtained solutions for both small and large values of λ. Lin and Chao [5] performed series solution to analyze the free convection flow over two-dimensional and axisymmetric bodies of arbitrary geometry. Moreover, Merkin [6] studied the free convection from elliptic cylinders while Ingham [7] illustrated the previous problem for an unsteady flow past as isothermal horizontal cylinder. Badr [8] accomplished a theoretical investigation to expose the features of laminar mixed convection from a horizontal cylinder. In order to materialize the target, the Grashof number and Reynolds number are assumed to be large while the Prandtl number is kept constant. He also considered the same problem for both parallel and contra flows [9].

Hossain et al. [10] considered the combined convection from a horizontal circular cylinder subjected to the radiation conduction interaction. On the contrary, Aldoss et al. [11] examined magnetohydrodynamic mixed convection from a horizontal circular cylinder. However, Hossain et al. [12] examined the unsteady free convection flow over a vertical surface. Nazar et al. [13] studied the effect of buoyancy force resulting from a horizontal circular cylinder subjected to thermal heat flux condition. The same group has considered the similar problem for an isothermal horizontal circular cylinder [14]. Furthermore, Molla et al. [15] examined the free convection flow from a horizontal cylinder under the influence of uniform heat flux and heat generation. Cheng [16] has taken the same problem for elliptic type cylinder where the resulting non-linear equations were solved numerically by cubic spilling collocation method. Almost a decade ago, Hossain et al. [17] analyzed a free convection problem due to fluctuations in temperature along a horizontal circular cylinder. Begum et al. [18] examined the heat transfer and separation characteristics due to natural convection from a rotating round-nosed body. Results are discussed with the skin friction and heat transfer taking different Prandtl number and power-law index. Hossain et al. [19] investigated the mixed convective flow of dusty fluid past a vertical wedge subject to the fluctuating free stream and surface temperature. The skin friction and heat transfer have been illustrated with the change of the ratio of the particle density to the gas density and the Richardson's number.

Ali et al. [20] numerically investigated the mixed convection flow from a circular cylinder which is embedded in an impulsive free stream flow of a micropolar fluid. The mixed convection flow from a circular cylinder was numerically examined by Nazar et al. [21]. In this case, the cylinder was assumed in a porous medium filled with nanofluid. Sarif et al. [22] studied the combined effect of free and forced convection flow over a horizontal circular cylinder subjected to convective boundary condition. However, Kamrujjaman et al. [23] considered mixed convection problem for a horizontal cylinder. They have considered small amplitude oscillations in surface temperature and free stream velocity. Very recently, Roy and Hossain [24] have revealed the flow and heat transfer of mixed convection flow past a permeable sphere while Roy et al. [25] have examined the similar characteristics of compressible fluid past a heated cylinder.

From the above literature survey, it is evident that no study has taken an attempt to investigate the boundary layer separation of incompressible mixed convection flow past a cylinder. Thus, the objective of this study is to reveal the boundary layer characteristics of mixed convection flow past an isothermal circular cylinder. Adopting an appropriate transformation,

the problem is presented as a system of dimensionless equations. We solve this system utilizing finite difference scheme for all time regime and series solution for small time regime and local non-similarity technique for long time regime. Results are presented to expose the effects of Prandtl number, Pr, and Richardson number, λ on the local friction factor and heat transfer. Moreover, the variations of streamlines and isotherms for different Prandtl number and Richardson number are demonstrated which clearly show how the point of separation of the boundary layer depends on these parameters.

Formulation of the Problem

We consider a two-dimensional, unsteady and mixed convection boundary layer flow of an incompressible fluid past an isothermal circular cylinder. Figure 1 illustrates the flow configuration and the coordinate system of the problem. In this study, we assume Boussinesq approximations in which the variable properties of the fluid have been neglected but appeared in the term multiplied by g, the acceleration due to gravity. Under the above assumptions, the boundary layer equations for the problem are [14]:

$$\frac{\partial u}{\partial x}+\frac{\partial v}{\partial y}=0 \tag{1}$$

$$\frac{\partial u}{\partial t}+u\frac{\partial u}{\partial x}+v\frac{\partial u}{\partial y}=U_e\frac{dU_e}{dx}+\nu\frac{\partial^2 u}{\partial y^2}+g\beta(T-T_\infty)\sin\left(\frac{x}{r}\right) \tag{2}$$

$$\rho C_p\left(\frac{\partial T}{\partial t}+u\frac{\partial T}{\partial x}+v\frac{\partial T}{\partial y}\right)=\kappa\frac{\partial^2 T}{\partial y^2} \tag{3}$$

where x is the distance along the stream-wise direction and y is the normal direction to the cylinder surface, u and v the velocity components in x and y directions respectively, κ the thermal conductivity, β the coefficient of thermal expansion, ν the kinematic viscosity, ρ the fluid density, T the temperature of the fluid, T_∞ the ambient temperature of the fluid, g the gravitational acceleration, C_p the specific heat at constant pressure, r the radius of the circular cylinder, $U_e(x)$ the external velocity of the fluid and t is the time.

The boundary conditions for this model are,

$$\begin{aligned} y=0:\ u=v=0,\ T=T_w \\ y\to\infty: u=U_e(x)=U_\infty\sin(x/r),\ T=T_\infty \end{aligned} \tag{4}$$

In Eq. (2), the pressure term is represented in terms of the external velocity $U_e(x)$. Also the free convective term $g\beta(T-T_\infty)\sin(x/r)$ accounts for the buoyancy force under the Boussinesq approximation. The ambient velocity of the fluid is denoted by U_∞, which is known as the free stream velocity. The direction of this velocity is assumed to be vertically upward from the horizontal circular cylinder so that the boundary layer flow velocity becomes $U_\infty\sin(x/r)$. The average surface temperature of the cylinder is maintained at ΔT, where, $\Delta T = T_w - T_\infty$.

Now we bring in the following group of non-dimensional variables

$$\begin{aligned} u=\frac{\nu}{r}\mathrm{Re}U,\quad v=\frac{\nu}{r}\mathrm{Re}^{1/2}V,\quad S=\frac{T-T_\infty}{\Delta T} \\ X=\frac{x}{r},\quad Y=\mathrm{Re}^{1/2}\frac{y}{r},\quad \zeta=\frac{\nu\mathrm{Re}}{r^2}t \end{aligned} \tag{5}$$

where the Reynolds number is denoted by Re and defined as $Re = U_\infty r/\nu$ and ζ represents the dimensionless time.

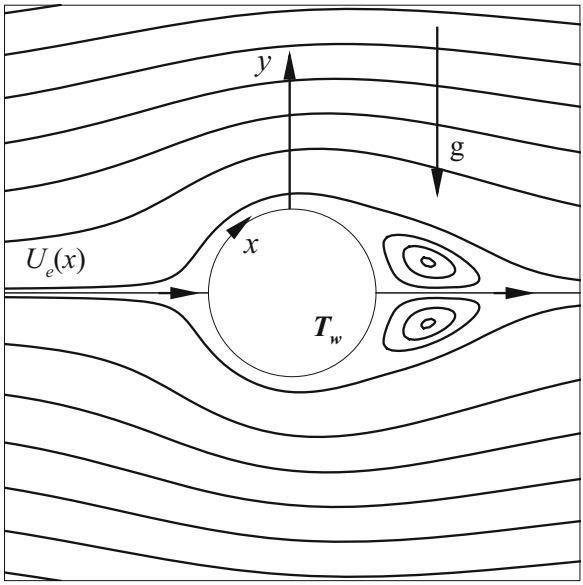

Fig. 1 Physical model with coordinate system

The use of the relations (5) into Eqs. (1)–(3) yields

$$\frac{\partial U}{\partial X} + \frac{\partial V}{\partial Y} = 0 \tag{6}$$

$$\frac{\partial U}{\partial \zeta} + U\frac{\partial U}{\partial X} + V\frac{\partial U}{\partial Y} = \sin X \cos X + \lambda S \sin X + \frac{\partial^2 U}{\partial Y^2} \tag{7}$$

$$\frac{\partial S}{\partial \zeta} + U\frac{\partial S}{\partial X} + V\frac{\partial S}{\partial Y} = \frac{1}{\Pr}\frac{\partial^2 S}{\partial Y^2} \tag{8}$$

The boundary conditions (4) are then reduced to

$$\begin{aligned} Y = 0 : U = V = 0, \quad S = 1 \\ Y \to \infty : U = U_e(X), \quad S = 0 \end{aligned} \tag{9}$$

Here, $\Pr = \nu/\alpha$ is the Prandtl number and $\lambda = Gr/Re^2$ is the buoyancy parameter, where $Gr = g\beta r^3 \Delta T/\nu^2$ is the Grashof number. The parameters Gr and Re indicate whether the flow is laminar or turbulent and free convective. The buoyancy parameter, λ, is dimensionless and also known as a mixed convection parameter. When $\lambda \gg 1$, the natural or free convection dominates while $\lambda \ll 1$ indicating the forced convection. But $\lambda \approx 1$, defines the characteristic for mixed convection flow. Since we consider the circular cylinder is heated then $\Delta T > 0$ which implies also $\lambda > 0$. In this case, both the forced and free convection boundary layers begin from the stagnation point and the boundary layer is increased due to the positive value of buoyancy force as $\lambda > 0$.

Methods of Solution

In this study, we utilize finite difference method valid for all time to solve the Eqs. (7)–(9). In order to validate the numerical solutions, we also solve the equations using the perturbation

method for small time and the asymptotic method for long time. The aforesaid methods of solution have been elucidated in the following sub-sections.

Stream Function Formulation

To reduce the set of Eqs. (7) and (8) to a compatible form for numerical integration, we use the transformations,

$$\psi = (1+\mathrm{Pr})^{-3/4}(1-e^{-\zeta})^{1/2}\sin X\ F(\zeta, X, \eta),$$
$$\eta = (1+\mathrm{Pr})^{1/4}(1-e^{-\zeta})^{-1/2}Y, \quad S = \theta(\zeta, X, \eta) \tag{10}$$

where ψ is the stream function, η and ζ are the dimensionless time and similarity variable, and F and θ are the dimensionless stream function and temperature function, respectively. The stream function ψ, defined from the continuity Eq. (7) is,

$$U = \frac{\partial \psi}{\partial Y} \quad \text{and} \quad V = -\frac{\partial \psi}{\partial X} \tag{11}$$

Thus we obtain the following Eqs. (12)–(20) by using the above transformations,

$$\frac{\partial U}{\partial \zeta} = (1+\mathrm{Pr})^{-1/2}\sin X\left\{\frac{\partial F'}{\partial \zeta} - \frac{1}{2}e^{-\zeta}\left(1-e^{-\zeta}\right)^{-1}\eta F''\right\} \tag{12}$$

$$U\frac{\partial U}{\partial X} = (1+\mathrm{Pr})^{-1}\sin X\left\{\sin X F'\frac{\partial F'}{\partial X} + \cos X F'^2\right\} \tag{13}$$

$$V\frac{\partial U}{\partial Y} = -(1+\mathrm{Pr})^{-1}\sin X\left\{\sin X F''\frac{\partial F}{\partial X} + \cos X F F''\right\} \tag{14}$$

$$\frac{\partial^2 U}{\partial Y^2} = \left(1-e^{-\zeta}\right)^{-1}\sin X F''' \tag{15}$$

$$\frac{\partial S}{\partial \zeta} = \frac{\partial \theta}{\partial \zeta} - \frac{1}{2}e^{-\zeta}\left(1-e^{-\zeta}\right)^{-1}\eta\theta' \tag{16}$$

$$U\frac{\partial S}{\partial X} = (1+\mathrm{Pr})^{-1/2}\sin X F'\frac{\partial \theta}{\partial X} \tag{17}$$

$$V\frac{\partial S}{\partial Y} = -(1+\mathrm{Pr})^{-1/2}\theta'\left\{\sin X\frac{\partial F}{\partial X} + \cos X F\right\} \tag{18}$$

$$\frac{\partial^2 S}{\partial Y^2} = (1+\mathrm{Pr})^{1/2}\left(1-e^{-\zeta}\right)^{-1}\theta'' \tag{19}$$

Upon substitution the Eqs. (12)–(19) into Eqs. (7)–(8), we obtain

$$\begin{aligned}(1+\mathrm{Pr})F''' + \frac{1}{2}\sqrt{1+\mathrm{Pr}}e^{-\zeta}\eta F'' + (1-e^{-\zeta})\cos X\left(FF'' - F'^2\right) + (1+\mathrm{Pr})(1-e^{-\zeta})\cos X \\ = \sqrt{1+\mathrm{Pr}}(1-e^{-\zeta})\frac{\partial F'}{\partial \zeta} + (1-e^{-\zeta})\sin X\left(F'\frac{\partial F'}{\partial X} - F''\frac{\partial F}{\partial X}\right) - (1+\mathrm{Pr})(1-e^{-\zeta})\lambda\theta\end{aligned} \tag{20}$$

$$\begin{aligned}\frac{1+\mathrm{Pr}}{\mathrm{Pr}}\theta'' + \frac{1}{2}\sqrt{1+\mathrm{Pr}}e^{-\zeta}\eta\theta' + (1-e^{-\zeta})\cos X F\theta' = \sqrt{1+\mathrm{Pr}}(1-e^{-\zeta})\frac{\partial \theta}{\partial \zeta} \\ + (1-e^{-\zeta})\sin X\left(F'\frac{\partial \theta}{\partial X} - \theta'\frac{\partial F}{\partial X}\right)\end{aligned} \tag{21}$$

The associated boundary conditions are,

$$F(\zeta,0,X)=0,\quad F'(\zeta,0,X)=0,\quad \theta(\zeta,0,X)=1,$$
$$F'(\zeta,\infty,X)=\sqrt{1+\mathrm{Pr}},\quad \theta(\zeta,\infty,X)=0. \tag{22}$$

Here primes represent differentiation with respect to η.

Local Friction Factor and Rate of Heat Transfer

The local friction factor, τ_x, and the heat transfer rate, q_x, are two important physical quantities in fluid dynamics. These quantities are small when the convective flow moves away from the surface and are large when the normal velocity approaches the surface. These two parameters are defined as following:

$$\tau_x=\mu\left(\frac{\partial u}{\partial y}\right)_{y=0} \tag{23}$$

$$q_x=-\kappa\left(\frac{\partial T}{\partial y}\right)_{y=0} \tag{24}$$

Substituting Eqs. (5) and (10) into Eqs. (23)–(24) we get,

$$\tau_x=(1+\mathrm{Pr})^{-1/4}\left(1-e^{-\zeta}\right)^{-1/2}\sin X F''(\zeta,0,X) \tag{25}$$

$$q_x=-(1+\mathrm{Pr})^{1/4}\left(1-e^{-\zeta}\right)^{-1/2}\theta'(\zeta,0,X) \tag{26}$$

Knowing the values of $F''(\zeta,0,X)$ and $\theta'(\zeta,0,X)$ from the Eqs. (20)–(21) using Eq. (22), one can easily obtains the local friction factor and heat transfer rate from the Eqs. (25)–(26).

Perturbation Solutions for Small Time Regime ($\zeta \ll 1$)

At small time region Eqs. (20) and (21) must be transformed into a suitable form for analysis. When $\zeta \ll 1$, the values of $e^{-\zeta}\approx 1$ and $1-e^{-\zeta}\approx\zeta$. Consequently, the Eqs. (20)–(21) are reduced to,

$$(1+\mathrm{Pr})F'''+\frac{1}{2}\sqrt{1+\mathrm{Pr}}\eta F''+\zeta\cos X\left(FF''-F'^2\right)+(1+\mathrm{Pr})\zeta\cos X$$
$$=\sqrt{1+\mathrm{Pr}}\zeta\frac{\partial F'}{\partial\zeta}+\zeta\sin X\left(F'\frac{\partial F'}{\partial X}-F''\frac{\partial F}{\partial X}\right)-(1+\mathrm{Pr})\zeta\lambda\theta \tag{27}$$

$$\frac{1+\mathrm{Pr}}{\mathrm{Pr}}\theta''+\frac{1}{2}\sqrt{1+\mathrm{Pr}}\eta\theta'+\zeta\cos X F\theta'=\sqrt{1+\mathrm{Pr}}\zeta\frac{\partial\theta}{\partial\zeta}+\zeta\sin X\left(F'\frac{\partial\theta}{\partial X}-\theta'\frac{\partial F}{\partial X}\right) \tag{28}$$

The corresponding boundary conditions are,

$$F(\zeta,0,X)=0,\quad F'(\zeta,0,X)=0,\quad \theta(\zeta,0,X)=1$$
$$F'(\zeta,\infty,X)=\sqrt{1+\mathrm{Pr}},\quad \theta(\zeta,\infty,X)=0 \tag{29}$$

For small values of ζ ($\gg 1$) we get the following equation by expanding the functions F and θ in powers of ζ:

$$F=\sum_{i=0}^{\infty}\zeta^i F_i\quad\text{and}\quad\theta=\sum_{i=0}^{\infty}\zeta^i\theta_i \tag{30}$$

Using the expressions of (30) into the Eqs. (27) and (28) and equating the coefficients of ζ up to second order, we have

Equations of $O(\zeta^0)$:

$$(1+\mathrm{Pr})F_0''' + \frac{1}{2}\sqrt{1+\mathrm{Pr}}\eta F_0'' = 0 \tag{31}$$

$$\frac{1+\mathrm{Pr}}{\mathrm{Pr}}\theta_0'' + \frac{1}{2}\sqrt{1+\mathrm{Pr}}\eta\theta_0' = 0 \tag{32}$$

$$F_0(0,X) = 0, \quad F_0'(0,X) = 0, \quad \theta_0(0,X) = 1,$$
$$F_0'(\infty,X) = \sqrt{1+\mathrm{Pr}}, \quad \theta_0(\infty,X) = 0 \tag{33}$$

Equations of $O(\zeta^1)$:

$$(1+\mathrm{Pr})F_1''' + \sqrt{1+\mathrm{Pr}}\left(\frac{1}{2}\eta F_1'' - F_1'\right) + \cos X\left(F_0F_0'' - F_0'^2\right)$$
$$+ (1+\mathrm{Pr})\cos X + (1+\mathrm{Pr})\lambda\theta_0 = 0 \tag{34}$$

$$\frac{1+\mathrm{Pr}}{\mathrm{Pr}}\theta_1'' + 1 + \mathrm{Pr}\left(\frac{1}{2}\eta\theta_1' - \theta_1\right) + \cos X F_0\theta_0' = 0 \tag{35}$$

$$F_1(0,X) = 0, \quad F_1'(0,X) = 0, \quad \theta_1(0,X) = 0,$$
$$F_1'(\infty,X) = 0, \quad \theta_1(\infty,X) = 0 \tag{36}$$

Equations of $O(\zeta^2)$:

$$(1+\mathrm{Pr})F_2''' + \sqrt{1+\mathrm{Pr}}\left(\frac{1}{2}\eta F_2'' - 2F_2'\right)$$
$$+ \cos X\left(F_0F_1'' + F_1F_0'' - 2F_0'F_1'\right) + (1+\mathrm{Pr})\lambda\theta_1 = 0 \tag{37}$$

$$\frac{1+\mathrm{Pr}}{\mathrm{Pr}}\theta_2'' + \sqrt{1+\mathrm{Pr}}\left(\frac{1}{2}\eta\theta_2' - 2\theta_2\right) + \cos X\left(F_0\theta_1' + F_1\theta_0'\right) = 0 \tag{38}$$

$$F_2(0,X) = 0, \quad F_2'(0,X) = 0, \quad \theta_2(0,X) = 0,$$
$$F_2'(\infty,X) = 0, \quad \theta_2(\infty,X) = 0 \tag{39}$$

We solve each of the above system of equations using non-linear shooting method. When the values of $F_i''(0,X)$ and $\theta_i'(0,X)$ for $i = 0, 1, 2$, are determined, we can readily find the values of the local friction factor and the local rate of heat transfer using the following relations:

$$\tau_x = (1+\mathrm{Pr})^{-1/4}\left(1-e^{-\zeta}\right)^{-1/2}\sin X\sum_{i=0}^{\infty}\zeta^i F_i \tag{40}$$

$$q_x = -(1+\mathrm{Pr})^{1/4}\left(1-e^{-\zeta}\right)^{-1/2}\sum_{i=0}^{\infty}\zeta^i\theta_i \tag{41}$$

Asymptotic Solutions for Long Time Regime ($\zeta \gg 1$)

Now we seek the solutions of Eqs. (20) and (21) for long time regime, ζ ($\gg 1$). When $\zeta \gg 1$, the values become $e^{-\zeta} \approx \zeta^{-1}$ and $(1-e^{-\zeta}) \approx 1-\zeta^{-1}$. The Eqs. (20) and (21) thus reduce to

$$(1+\mathrm{Pr})F''' + \frac{1}{2}\sqrt{1+\mathrm{Pr}}\zeta^{-1}\eta F'' + \left(1-\zeta^{-1}\right)\cos X\left(FF'' - F'^2\right) + (1+\mathrm{Pr})\left(1-\zeta^{-1}\right)\cos X$$
$$= \sqrt{1+\mathrm{Pr}}\left(1-\zeta^{-1}\right)\frac{\partial F'}{\partial \zeta} + \left(1-\zeta^{-1}\right)\sin X\left(F'\frac{\partial F'}{\partial X} - F''\frac{\partial F}{\partial X}\right) - (1+\mathrm{Pr})\left(1-\zeta^{-1}\right)\lambda\theta \tag{42}$$

$$\frac{1+\mathrm{Pr}}{\mathrm{Pr}}\theta'' + \frac{1}{2}\sqrt{1+\mathrm{Pr}}\zeta^{-1}\eta\theta' + \left(1-\zeta^{-1}\right)\cos X F\theta' = \sqrt{1+\mathrm{Pr}}\left(1-\zeta^{-1}\right)\frac{\partial\theta}{\partial\zeta}$$
$$+ \left(1-\zeta^{-1}\right)\sin X\left(F'\frac{\partial\theta}{\partial X} - \theta'\frac{\partial F}{\partial X}\right) \tag{43}$$

The boundary conditions then turn into the following form,

$$F(\zeta,0,X) = 0, \quad F'(\zeta,0,X) = 0, \quad \theta(\zeta,0,X) = 1$$
$$F'(\zeta,\infty,X) = \sqrt{1+\mathrm{Pr}}, \quad \theta(\zeta,\infty,X) = 0 \tag{44}$$

Let us expand the functions F and θ in powers of ζ as,

$$F = \sum_{i=0}^{\infty}\zeta^{-i}F_i, \quad \theta = \sum_{i=0}^{\infty}\zeta^{-i}\theta_i \tag{45}$$

Combining the Eqs. (45) with (42) and (43), the coefficients of ζ^0 yields,

$$(1+\mathrm{Pr})F_0''' + \cos X\left(F_0F_0'' - F_0'^2\right) + (1+\mathrm{Pr})\cos X + (1+\mathrm{Pr})\lambda\theta_0$$
$$= \sin X\left(F_0'\frac{\partial F_0'}{\partial X} - F_0''\frac{\partial F_0}{\partial X}\right) \tag{46}$$

$$\frac{1+\mathrm{Pr}}{\mathrm{Pr}}\theta_0'' + \cos X F_0\theta_0' = \sin X\left(F_0'\frac{\partial\theta_0}{\partial X} - \theta_0'\frac{\partial F_0}{\partial X}\right) \tag{47}$$

The associated boundary conditions are

$$F_0(0,X) = 0, \quad F_0'(0,X) = 0, \quad \theta_0(0,X) = 1$$
$$F_0'(\infty,X) = \sqrt{1+\mathrm{Pr}}, \quad \theta_0(\infty,X) = 0 \tag{48}$$

It is evident that the Eqs. (42) and (43) are coupled and so these are solved using local non-similarity method. Accordingly, we rewrite the equations using the relations,

$$\frac{\partial F_0}{\partial X} = z, \quad \frac{\partial F_0'}{\partial X} = z', \quad \frac{\partial\theta_0}{\partial X} = \phi. \tag{49}$$

Thus the Eqs. (46)–(47) turn into the form,

$$(1+\mathrm{Pr})F_0''' + \cos X\left(F_0F_0'' - F_0'^2\right) + (1+\mathrm{Pr})\cos X + (1+\mathrm{Pr})\lambda\theta_0 = \sin X\left(F_0'z' - F_0''z\right) \tag{50}$$

$$\frac{1+\mathrm{Pr}}{\mathrm{Pr}}\theta_0'' + \cos X F_0\theta_0' = \sin X\left(F_0'\phi - \theta_0'z\right) \tag{51}$$

subject to the boundary conditions

$$z(0,X) = 0, \quad z'(0,X) = 0, \quad \phi(0,X) = 1$$
$$z'(\infty,X) = \sqrt{1+\mathrm{Pr}}, \quad \phi(\infty,X) = 0 \tag{52}$$

Differentiating the Eqs. (50)–(52) with respect to X, we get the desired equations with the boundary conditions,

$$(1+\mathrm{Pr})z''' + \cos X\left(F_0 z'' + zF_0'' - 2F_0' z'\right) - \sin X\left\{F_0 F_0'' - \left(F_0'\right)^2\right\} - (1+\mathrm{Pr})\sin X + (1+\mathrm{Pr})\lambda\phi = \sin X\left\{\left(z'\right)^2 - zz''\right\} + \cos X\left(F_0' z' - F_0'' z\right) \tag{53}$$

$$\frac{1+\mathrm{Pr}}{\mathrm{Pr}}\phi'' + \cos X\left(F_0\phi' + \theta_0' z\right) - \sin X F_0\theta_0' = \sin X\left(z'\phi - z\phi'\right) + \cos X\left(F_0'\phi - \theta_0' z\right) \tag{54}$$

$$z'(0,X) = 0, \quad z''(0,X) = 0, \quad \phi'(0,X) = 0$$
$$z''(\infty,X) = 0, \quad \phi'(\infty,X) = 0 \tag{55}$$

Here the Eqs. (50)–(55) is a system of coupled ordinary differential equations. We perform the local non-similarity method to solve these equations. Thus the local friction factor and the rate of heat transfer valid for the long time are determined using the expressions,

$$\tau_x = (1+\mathrm{Pr})^{-1/4}\left(1-e^{-\zeta}\right)^{-1/2}\sin X\, F_0''(0,X) \tag{56}$$

$$q_x = -(1+\mathrm{Pr})^{1/4}\left(1-e^{-\zeta}\right)^{-1/2}\theta_0'(0,X) \tag{57}$$

Numerical Solutions for Any Time, ζ

The stream function formulation is used for the solution of entire time. Here the Eqs. (20)–(22) will solve by using finite difference method. In this process, we first transform the partial differential Eqs. (20)–(22) into the second order differential equations by taking the following assumptions,

$$F' = u, \quad F = v \tag{58}$$

Substituting Eq. (58) into the Eqs. (20)–(22) we obtain,

$$(1+\mathrm{Pr})u'' + \frac{1}{2}\sqrt{1+\mathrm{Pr}}\,p_1\eta u' + p_2\cos X\left(u'v - u^2\right) + (1+\mathrm{Pr})p_2\cos X = \sqrt{1+\mathrm{Pr}}\,p_2\frac{\partial u}{\partial\zeta} + p_2\sin X\left(u\frac{\partial u}{\partial X} - u'\frac{\partial v}{\partial X}\right) - (1+\mathrm{Pr})p_2\lambda\theta \tag{59}$$

$$\frac{1+\mathrm{Pr}}{\mathrm{Pr}}\theta'' + \frac{1}{2}\sqrt{1+\mathrm{Pr}}\,p_1\eta\theta' + p_2\cos X v\theta' = \sqrt{1+\mathrm{Pr}}\,p_2\frac{\partial\theta}{\partial\zeta} + p_2\sin X\left(u\frac{\partial\theta}{\partial X} - \theta'\frac{\partial v}{\partial X}\right) \tag{60}$$

$$v(\zeta,0,X) = 0, \quad u(\zeta,0,X) = 0, \quad \theta(\zeta,0,X) = 1$$
$$u(\zeta,\infty,X) = \sqrt{1+\mathrm{Pr}}, \quad \theta(\zeta,\infty,X) = 0 \tag{61}$$

In the above equations, we assume

$$p_1 = e^{-\zeta} \quad \text{and} \quad p_2 = \left(1-e^{-\zeta}\right). \tag{62}$$

Now we employ finite difference technique to solve the Eqs. (59)–(60) with boundary conditions (61). In the present method, we use central difference formula along η-direction and backward difference formula in X- and ζ-directions. In this way, the following system of tri-diagonal equations yields

$$B_k W^n_{i,j-1} + A_k W^n_{i,j} + C_k W^n_{i,j+1} = D_k. \tag{63}$$

Here, the subscript k (= 1, 2) indicates the momentum equation and the energy equation as well as the functions F and θ, respectively. Also i (= 1, 2, 3,…, M) and j (= 1, 2, 3,…, N) represent the mesh points in X and η-directions, respectively while the superscript n (=

1, 2, 3,…, K) is the mesh point in ζ-direction. In Eq. (63), the coefficients A_k, B_k, C_k, D_k are given as below:

$$A_1 = 2(1+\mathrm{Pr}) + (\Delta\eta)^2 p_2 \left\{ \left(\cos X + \frac{\sin X}{\Delta X} \right) u^n_{2,j} + \frac{\sqrt{1+\mathrm{Pr}}}{\Delta\zeta} \right\} \tag{64}$$

$$B_1 = -(1+\mathrm{Pr}) - \frac{\Delta\eta}{2} \left\{ \frac{p_1}{2}\sqrt{1+\mathrm{Pr}}\left(\eta_j + \eta_{j-1}\right) + p_2 \left(\cos X v^n_{2,j} + \sin X \frac{v^n_{2,j} - v^n_{1,j}}{\Delta X} \right) \right\} \tag{65}$$

$$C_1 = -(1+\mathrm{Pr}) + \frac{\Delta\eta}{2} \left\{ \frac{p_1}{2}\sqrt{1+\mathrm{Pr}}\left(\eta_j + \eta_{j-1}\right) + p_2 \left(\cos X v^n_{2,j} + \sin X \frac{v^n_{2,j} - v^n_{1,j}}{\Delta X} \right) \right\} \tag{66}$$

$$D_1 = (\Delta\eta)^2 p_2 \left\{ \sqrt{1+\mathrm{Pr}} \frac{u^{n-1}_{2,j}}{\Delta\zeta} + \frac{\sin X u^n_{2,j} u^n_{1,j}}{\Delta X} + (1+\mathrm{Pr})\left(\cos X + \lambda\theta^n_{2,j} \right) \right\} \tag{67}$$

$$A_2 = \frac{2(1+\mathrm{Pr})}{\mathrm{Pr}} + (\Delta\eta)^2 p_2 \left\{ \sqrt{1+\mathrm{Pr}} \frac{1}{\Delta\zeta} + \frac{\sin X u^n_{2,j}}{\Delta X} \right\} \tag{68}$$

$$B_2 = -\frac{(1+\mathrm{Pr})}{\mathrm{Pr}} - \frac{\Delta\eta}{2} \left\{ \frac{p_1}{2}\sqrt{1+\mathrm{Pr}}\left(\eta_j + \eta_{j-1}\right) + p_2 \left(\cos X v^n_{2,j} + \sin X \frac{v^n_{2,j} - v^n_{1,j}}{\Delta X} \right) \right\} \tag{69}$$

$$C_2 = -\frac{(1+\mathrm{Pr})}{\mathrm{Pr}} + \frac{\Delta\eta}{2} \left\{ \frac{p_1}{2}\sqrt{1+\mathrm{Pr}}\left(\eta_j + \eta_{j-1}\right) + p_2 \left(\cos X v^n_{2,j} + \sin X \frac{v^n_{2,j} - v^n_{1,j}}{\Delta X} \right) \right\} \tag{70}$$

$$D_2 = (\Delta\eta)^2 p_2 \left(\sqrt{1+\mathrm{Pr}} \frac{\theta^{n-1}_{2,j}}{\Delta\zeta} + \frac{\sin X u^n_{2,j} \theta^n_{1,j}}{\Delta X} \right) \tag{71}$$

Keeping j and n fixed, the tri-diagonal system (63) is solved for i (= 1, 2, 3,…, M) by the use of Thomas Algorithm [26]. The solution procedure is then marched into j direction and finally in n direction. Until the solutions become steady state they are calculated at every step of time starting from $\zeta = 0.0$. The convergence property for the numerical solutions is determined when the variations of the values of the function $F(\zeta, \eta, X)$ in two successive iterations is smaller than 0.00001. In the X-direction the calculation is initiated from $X=$ 0.0 and then moves to the point $X=\pi$. For the present numerical simulation, we consider the step sizes as $\Delta X = \pi/360$, $\Delta Y = 0.02$, $\Delta\zeta = 0.01$ so that the solutions become grid independent. From Eqs. (59) and (60), we first determine the values of $(\partial u/\partial Y)_{Y=0}$ and $(\partial\theta/\partial Y)_{Y=0}$ and then calculate the local friction factor, τ_x and the rate of heat transfer, q_x using the following expressions:

$$\tau_x = (1+\mathrm{Pr})^{-1/4}\left(1 - e^{-\zeta}\right)^{-1/2} \sin X \left(\frac{\partial u}{\partial Y} \right)_{Y=0} \tag{72}$$

$$q_x = -(1+\mathrm{Pr})^{1/4}\left(1 - e^{-\zeta}\right)^{-1/2} \left(\frac{\partial\theta}{\partial Y} \right)_{Y=0} \tag{73}$$

Results and Discussion

In this study, the aim is to find out the effects of the variation of physical parameters such as Richardson number, λ, and the Prandtl number, Pr, on the fluid flow and heat transfer.

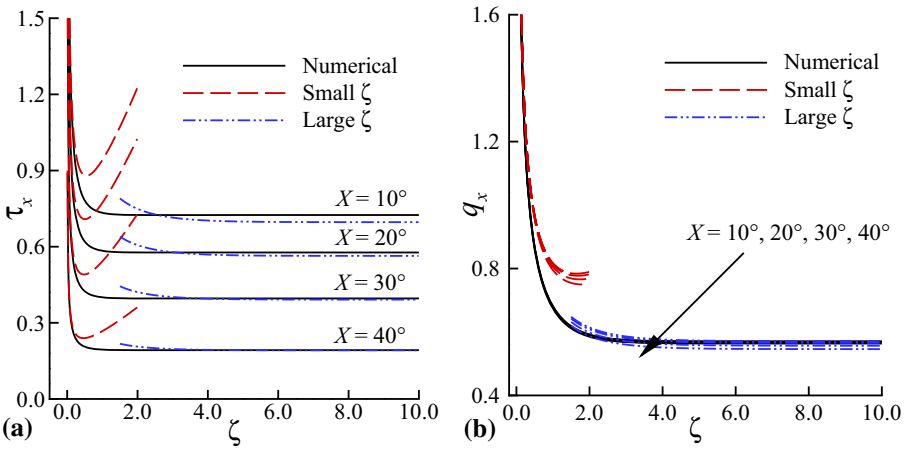

Fig. 2 Comparison of numerical and series solutions with **a** local friction factor and **b** heat transfer rate for Pr = 1.0 and $\lambda = 1.0$

Numerical solutions are illustrated with the local friction factor and local heat transfer rate as well as the streamlines and isotherms.

In order to confirm the accuracy of numerical solutions, we make a comparison of the local friction factor and the rate of heat transfer in Figs. 2a, b between the numerical solutions and the perturbation solutions for small time and the asymptotic solutions for long time. Figures indicate that the numerical solutions give a high degree of accuracy with the solutions for small time and long time.

In the following sections, the effects of relevant parameters using the numerical solutions have been demonstrated.

Local Friction Factor and Rate of Heat Transfer with the Change of Time (ζ)

The local friction factor and rate of heat transfer against X are shown in the Figs. 3a, b for different time, ζ. From the Fig. 3a we can observe that the local friction factor gradually increases with the increase of time, ζ, and becomes steady state at long time. There is a peak value near $X = 78^\circ$ for each corresponding time. The local friction factor increases along with the stream wise direction X, before it reaches the peak value and after the peak value the friction factor decreases gradually and try to reach steady state. The peak values of the local friction factor reduce with the increase of time, ζ. The reason behind this phenomenon is an abrupt upward evolution of the fluid when a heated cylinder is immersed in the fluid. When the evolution is accelerated then the fluid particles pass the cylinder keeping a distance and so the local friction factor decreases with the increasing value of X. The separation increases with the increasing value of time, ζ, since it is well observed from the Fig. 3a. For time $\zeta = 0.2$, there exists no separation point. When the steady state reaches, the values of local friction factor for different times overlap. From the Fig. 3b, it is clear that the rate of heat transfer decreases with the increasing value of time, ζ, and also the stream wise direction, X. Once it reaches steady state then all the values of heat transfer rate coincide.

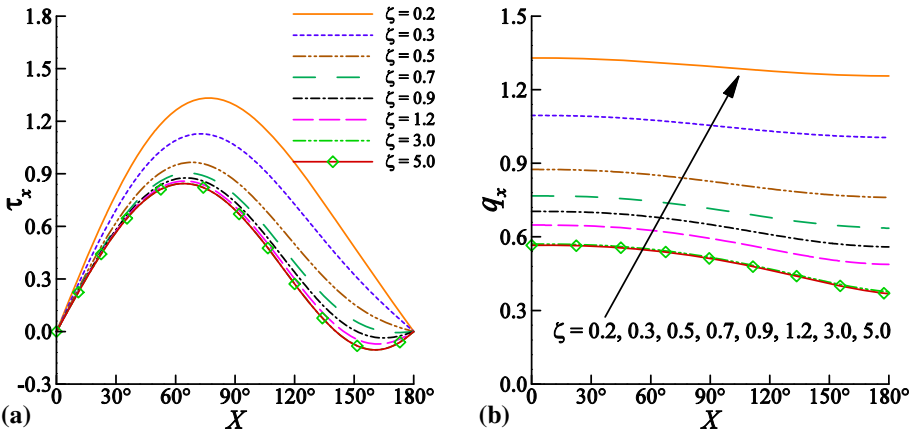

Fig. 3 **a** Local friction factor and **b** heat transfer rate for varying time, ζ, against X, for Pr = 1.0 and $\lambda = -0.1$

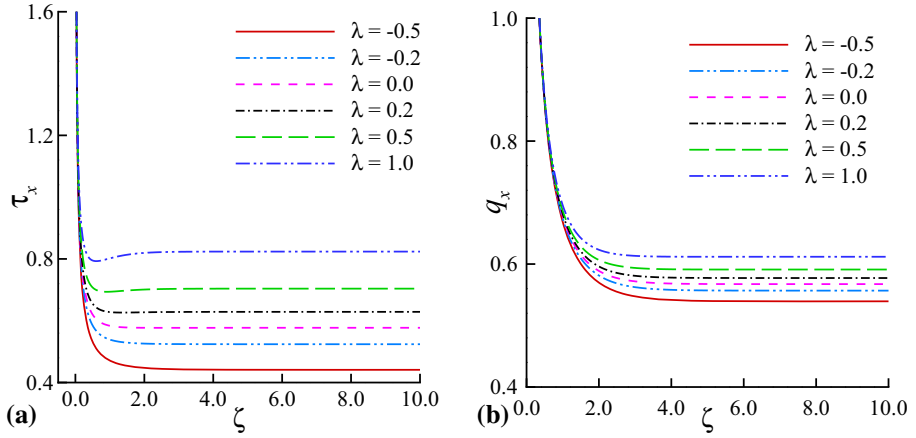

Fig. 4 **a** Local friction and **b** heat transfer rate against time, ζ, for different Richardson number, λ when $X =$ 30° and Pr = 1.0

Local Friction Factor and Rate of Heat Transfer for Different Richardson Number, λ

The variation in the local friction factor and rate of heat transfer against time, ζ, for different values of Richardson number, λ, are shown in Figs. 4a, b when Prandtl number, Pr = 1.0. Due to the increase of the Richardson number, λ, the local skin friction factor increases. The friction factor at first reduces and this reduction happens due to the positive value of Richardson number, λ. The effect of the positive value of λ appears to be a pressure gradient which results in higher fluid flow in the boundary layer. The heat transfer rate increases quickly with the ascending value of the Richardson number, λ. As it expedites the fluid flow in the boundary layer, the boundary layer becomes thin. There is a reason for comparatively weaker dependence of the heat transfer rate on the Richardson number, λ, because it occurs explicitly in the energy equation.

Figure 5a, b represent the effect of Richardson number, λ, on the local friction factor and heat transfer rate against X, when Pr = 1.0. The local friction factor increases with the

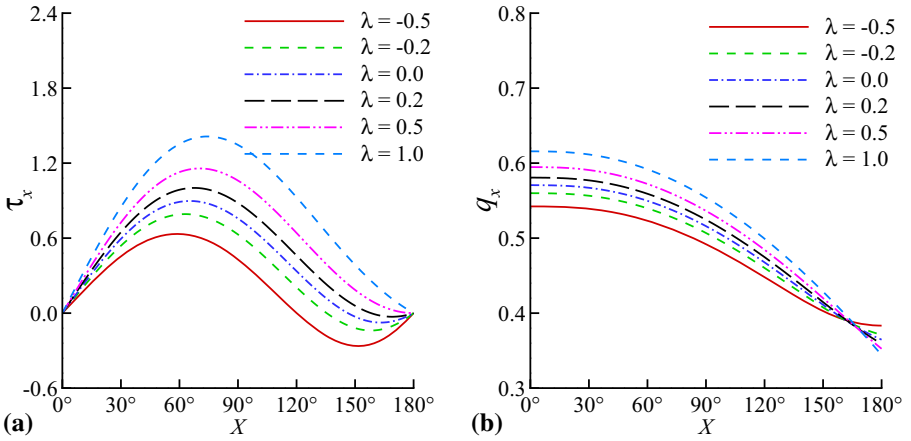

Fig. 5 **a** Local friction factor coefficient and **b** local Nusselt number against X for different Richardson number, λ when $\mathrm{Pr} = 1.0$

increasing value of λ while the separation point decreases. It is seen from the Fig. 5a that there is no point of separation for $\lambda \geq 0.2$. With the increase of the Richardson number, λ, the heat transfer rate also increases.

Effect of Prandtl Number, Pr, on the Local Friction Factor and Heat Transfer

The effect of the Prandtl number, Pr, on the local friction factor and heat transfer rate against time, ζ, is shown in Figs. 6a, b. It is seen that the local friction factor and heat transfer rate get steady state with the increase of time. For higher values of Prandtl number, Pr, the local friction factor decreases but the local heat transfer rate increases. Since the Prandtl number occurs explicitly in the energy equation, so the heat transfer rate has the effect more strongly than the friction factor. From the definition of Pr $(=\nu/\alpha)$, it is evident that the value of Pr is higher when the thermal diffusivity is smaller. This phenomenon indicates the decreasing energy transfer ability that causes the reduction of the thermal boundary layer.

Figures 7a, b depict the influence of Prandtl number, Pr, on the local friction factor and heat transfer rate against X. Results indicate that the friction factor increases with X and attains a peak value near the point $X = 72°$. It is evident from the friction factor profiles that for the Richardson number $\lambda = 1.0$, no separation point occurs for different values of Prandtl number. Besides, Fig. 7b shows that the rate of heat transfer significantly increases for higher values of Pr. It is noted that the effect of Pr on the rate of heat transfer appears to be stronger than on the local friction factor.

Effect of Different Time, ζ, on the Streamlines and Isotherms

The streamlines and isotherms of the fluid for different time, ζ, are shown in the Fig. 8. Here, we consider Prandtl number, $\mathrm{Pr} = 1.0$, Richardson number, $\lambda = -0.2$, and time, $\zeta = 0.5$, 1.0, 2.0, 3.0 and 5.0. From these figures, we observe that the point of separation delays with time while the area of the vortices increases with the increase of time until the steady state. After steady state the flow lines remain same. Contrary to this, the temperature of the fluid

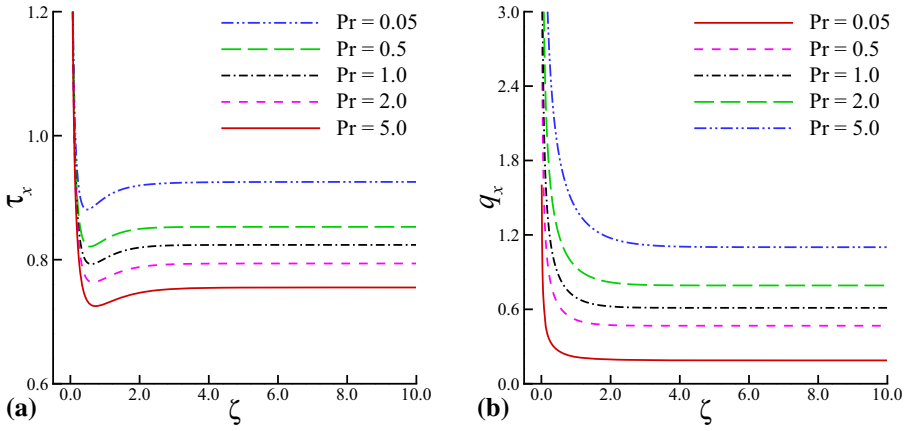

Fig. 6 **a** Local friction factor and **b** heat transfer rate against time, ζ for different Prandtl number, Pr, when $X = 30°$ and $\lambda = 1.0$

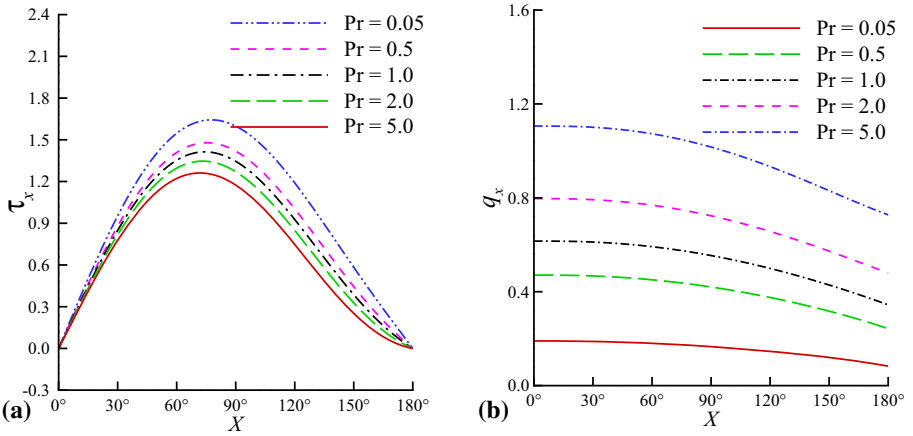

Fig. 7 **a** Local friction factor and **b** heat transfer rate against X, for different Prandtl number, Pr, when $\lambda = 1.0$

decreases with the increase of time. Here the boundary layer separation occurs mainly for the negative Richardson number, λ, because it causes dominating opposed forced convection flow.

Effect of Prandtl Number, Pr, on the Streamlines and Isotherms

Figure 9 illustrates the change of the streamlines and isotherms with the Prandtl number, Pr. These are significantly affected by the change of Pr. It is found that the point of separation diminishes for higher values of Prandtl number. Consequently, the size of the vortex decreases with it. Here, we consider the values of Prandtl number as, Pr = 0.72, 1.0, 3.0 and 5.0. For Pr = 0.72, the size of the vortex is large and so the separation point occurs earlier. But for large value of Prandtl number, the size of the vortex shrinks. Results also suggest that higher value of Pr significantly diminishes the thermal boundary layer.

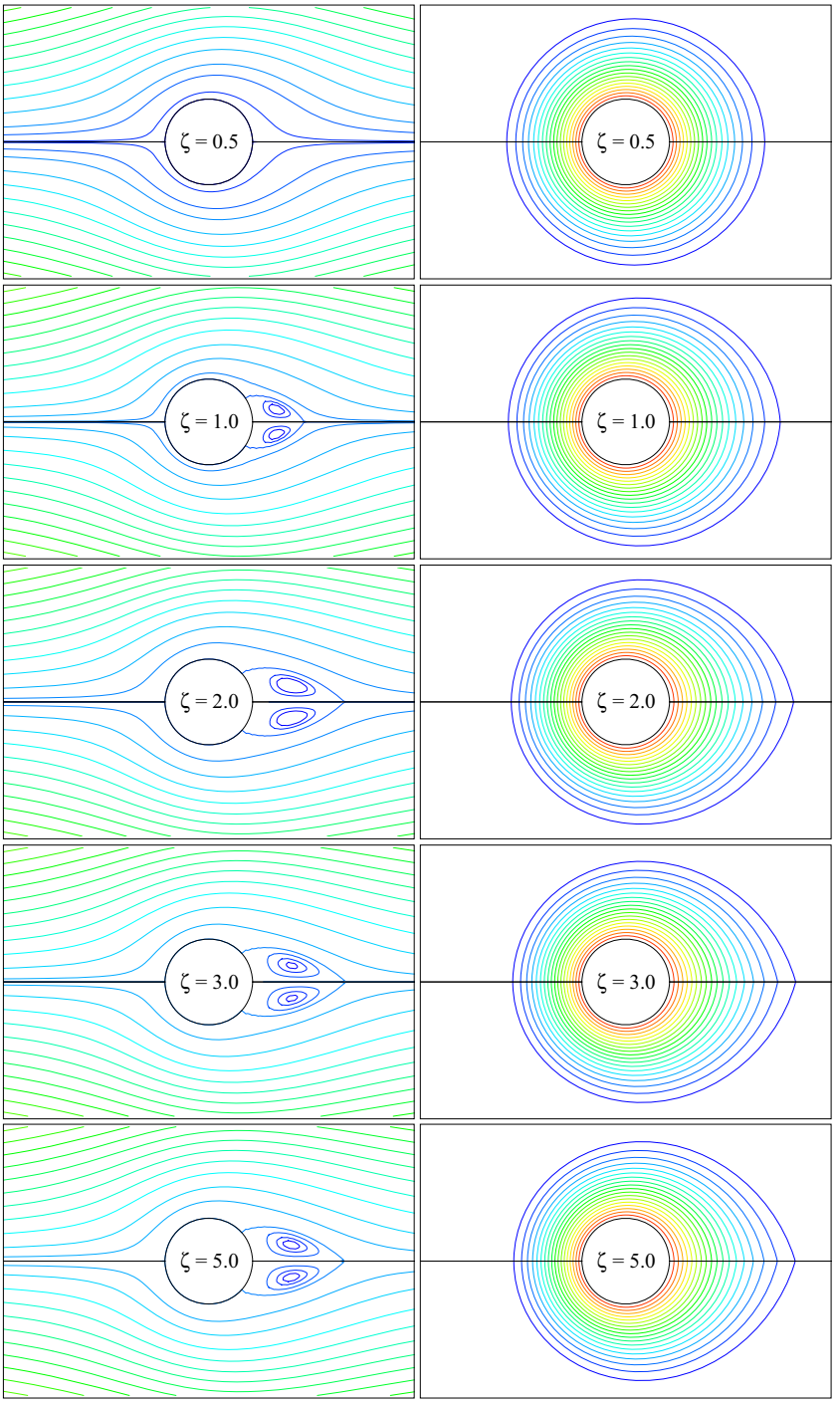

Fig. 8 Streamlines and isotherms for different values of time, ζ, when $\mathrm{Pr} = 1.0$ and $\lambda = -0.2$

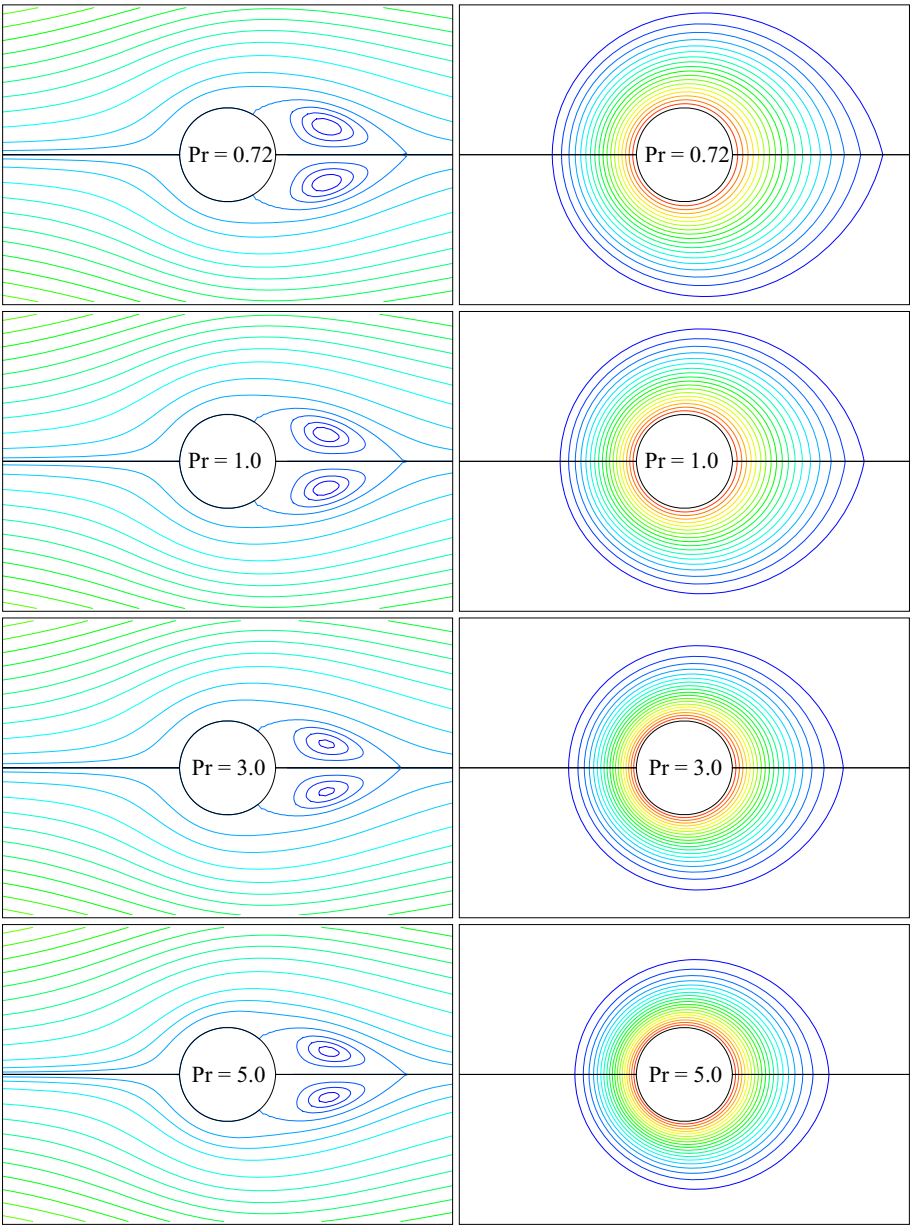

Fig. 9 Streamlines and isotherms for varying Prandtl number, Pr, when $\zeta = 10.0$ and $\lambda = -0.5$

Effect of Richardson Number, λ, on the Streamlines and Isotherms

Figure 10 shows the effect of Richardson number, λ, on the streamlines and isotherms for Pr $= 1.0$ at time, $\zeta = 10.0$. The influences of the increasing value of Richardson number occur in the area of the vortex. For higher values of Richardson number, the point of separation delays

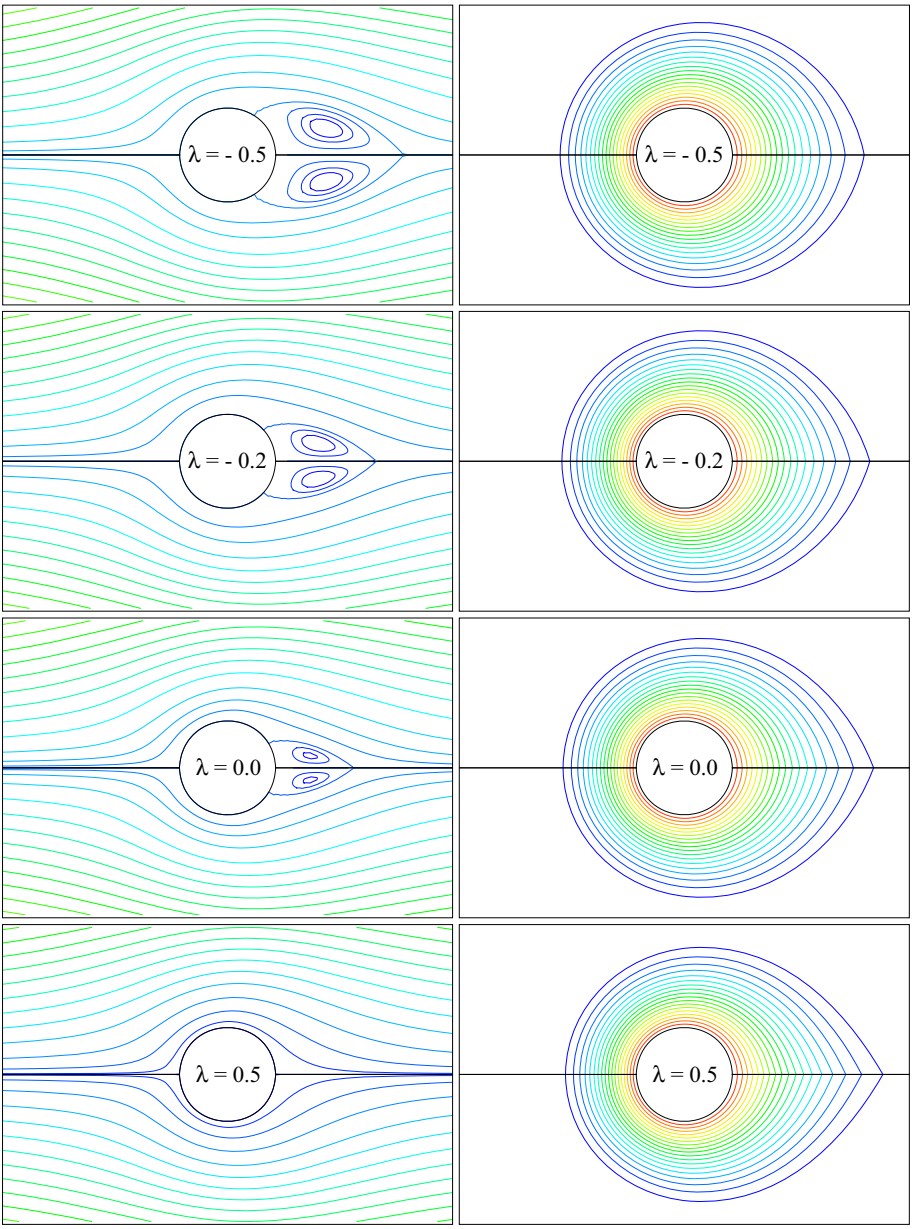

Fig. 10 Streamlines and isotherms for varying Richardson number, λ, when $\zeta = 10.0$ and $\mathrm{Pr} = 1.0$

and move to the rear stagnation point. As a result, the size of the vortex and the covering area decrease with it. Figure 10 also depicts that the temperature of the fluid increases with an increase of λ. It suggests that the thermal boundary layer thickens for higher Richardson number.

Conclusions

In this study, mixed convection flow past a heated circular cylinder has been investigated. The governing equations are made dimensionless using suitable transformations. Numerical results are determined using the finite difference method for any time as well as perturbation method for small time and local non-similarity method for large time. From the results illustrated above, the following conclusions are drawn:

- The local friction factor and heat transfer rate against time, ζ, increases with the augmented value of the Richardson number, λ. In this case, the momentum boundary layer is thick whereas the thermal boundary layer becomes thin. The remarkable finding is that the higher values of Richardson number delays the boundary-layer separation.
- The effect of Prandtl number, Pr, is quite prominent here. For increasing Pr the local heat transfer rate increases but the local friction factor decreases. It is found that the point of separation considerably decreases for higher values of Pr. Also the thermal boundary layer widens for increase of Pr.

References

1. Acrivos, A.: On the combined effect of forced and free convection heat transfer in laminar boundary layer flows. Chem. Eng. Sci. **21**, 343–352 (1966)
2. Sparrow, E.M., Lee, L.: Analysis of mixed convection about a horizontal cylinder. Int. J. Heat Mass Transf. **19**, 229–232 (1976)
3. Merkin, J.H.: Oscillatory free convection from an infinite horizontal cylinder. J. Fluid Mech. **30**, 561–575 (1967)
4. Merkin, J.H.: Mixed convection from a horizontal circular cylinder. Int. J. Heat Mass Transf. **20**, 73–77 (1977)
5. Lin, F.N., Chao, B.T.: Laminar free convection over two-dimensional and axisymmetric bodies of arbitrary contour. J. Heat Transf. **96**, 435–442 (1974)
6. Merkin, J.H.: Free convection boundary layers on cylinders of elliptic cross section. J. Heat Transf. **99**, 453–457 (1977)
7. Ingham, D.B.: Free-convection boundary layer on an isothermal horizontal cylinder. J. Appl. Math. Phys. **29**, 871–883 (1978)
8. Badr, H.M.: A theoretical study of laminar mixed convection from a horizontal cylinder in a cross stream. Int. J. Heat Mass Transf. **26**, 639–653 (1983)
9. Badr, H.M.: Laminar combined convection from a horizontal cylinder parallel and contra flow regimes. Int. J. Heat Mass Transf. **27**, 15–27 (1984)
10. Hossain, M.A., Kutubuddin, M., Pop, I.: Radiation–conduction interaction on mixed convection from a horizontal circular cylinder. Heat Mass Transf. **35**, 307–314 (1999)
11. Aldoss, T.K., Ali, Y.D., Al-Nimr, M.A.: MHD mixed convection from a horizontal circular cylinder. Numer. Heat Transf. **30**, 379–396 (1996)
12. Hossain, M.A., Hussain, S., Rees, D.A.S.: Influence of fluctuating surface temperature and concentration on natural convection flow from a vertical flat plate. J. Appl. Math. Mech. **81**, 699–709 (2001)
13. Nazar, R., Amin, N., Pop, I.: Free convection boundary layer flow on a horizontal circular cylinder with constant heat flux in a micro polar fluid. Int. J. Appl. Mech. Eng. **7**, 409–431 (2002)
14. Nazar, R., Amin, N., Pop, I.: Mixed convection boundary-layer flow from a horizontal circular cylinder with a constant surface heat flux. Heat Mass Transf. **40**, 219–227 (2004)
15. Molla, M.M., Paul, S.C., Hossain, M.A.: Natural convection flow from a horizontal circular cylinder with uniform heat flux in presence of heat generation. Appl. Math. Model. **33**, 3226–3236 (2009)
16. Cheng, C.Y.: Natural convection boundary layer on a horizontal elliptical cylinder with constant heat flux and internal heat generation. Int. Commun. Heat Mass Transf. **36**, 1025–1029 (2009)
17. Hossain, A., Kamrujjaman, M., Gorla, R.S.R.: Fluctuating free convection flow along heated horizontal circular cylinders. Int. J. Fluid Mech. Res. **36**, 207–230 (2009)

18. Begum, N., Siddiqa, S., Ouazzi, A., Hossain, M.A., Gorla, R.S.R.: Natural convection and separation points of a non-Newtonian fluid along a rotating round-nosed body. J. Therm. Heat Transf. **32**(4), 946–952 (2018)
19. Hossain, M.A., Roy, N.C., Siddiqa, S.: Unsteady mixed convection dusty fluid flow past a vertical wedge due to small fluctuation in free stream and surface temperature. Appl. Math. Comput. **293**, 480–492 (2017)
20. Ali, A., Amin, N., Pop, I.: Unsteady mixed convection boundary layer from a circular cylinder in a micro polar fluid. Int. J. Chem. Eng., Article ID 417875 (2010)
21. Nazar, R., Tham, L., Pop, I., Ingham, D.B.: Mixed convection boundary layer flow from a horizontal circular cylinder embedded in a porous medium filled with a nanofluid. Transp. Porous Media **86**, 517–536 (2011)
22. Sarif, N.M., Salleh, M.Z., Nazar, R.: Mixed convection flow over a horizontal circular cylinder in a viscous fluid at the lower stagnation point with convective boundary conditions. Sci. Asia **42**, 5–10 (2016)
23. Kamrujjaman, M., Hossain, M.A., Alam, J.: Mixed convection flow along a horizontal circular cylinder with small amplitude oscillation in surface temperature and free stream. Mech. Eng. Res. **6**, 34–47 (2016)
24. Roy, N.C., Hossain, M.A.: Unsteady magnetohydrodynamic mixed convection flow of micropolar fluid past a permeable sphere. J. Thermophys. Heat Transf. **31**, 686–699 (2017)
25. Roy, N.C., Rahman, T., Hossain, M.A., Gorla, R.S.R.: Boundary-layer characteristics of compressible flow past a heated cylinder with viscous dissipation. J. Thermophys. Heat Transf. **33**, 10–22 (2019)
26. Blottner, F.G.: Finite difference methods of solution of the boundary-layer equations. AIAA J. **8**, 193–205 (1970)